AIAA 80-1370R

Instantaneous Two-Dimensional Gas Concentration Measurements by Light Scattering

M. B. Long,* B. T. Chu,† and R. K. Chang†
Yale University, New Haven, Conn.

A light-scattering technique which makes it possible to map out the instantaneous concentration field at 10^4 points in a thin sheet intersecting a nonreacting turbulent flow is described. The concentration is inferred from the intensity of the Lorenz/Mie scattered radiation from a seeded flow. The signal is detected by a computer-controlled, low-light-level TV camera and the resulting data have the advantage of being both quantitative and visually interpretable. The technique can be modified to obtain temporal as well as spatial information. In addition, the use of other scattering mechanisms for similar measurements is discussed.

Introduction

WITH the realization of the importance of coherent structures in turbulent flows, there has been an increased interest in experimental means of obtaining information on the nature of these structures. The use of multipoint probes, conditional sampling techniques, and flow visualization has provided much new data. The picture is still incomplete, however, since most simultaneous multipoint measurements have been limited to a relatively small number of points, usually along a single line. Also, flow visualization, which provides a large amount of information, is generally only qualitative. In order to provide a large number of simultaneous, quantitative measurements, a nonintrusive light-scattering technique has been developed which makes it possible to measure gas concentration at 10,000 points within a plane intersecting a nonreacting turbulent flow.

The technique used is an extension of one first developed by Rosensweig[1] and later employed by several other researchers. A thorough review of the method has been given by Becker.[2] The technique is based on the fact that, if a gas is seeded with light-scattering particles having dimensions so small that there is negligible "slip" between the particles and the surrounding gas, each unit mass of the seeded gas will be marked by approximately the same number of aerosols in the course of its motion. (The size of the particles is sufficiently large so that there is negligible Brownian diffusion of particles due to molecular agitation. A precise estimate of how well the particles follow the fluid motion is given later.) If the seeded gas mixes with a second unseeded gas, the number of scattering particles in each unit volume of the mixture will be reduced and the scattered radiation will be proportionally less. Early experiments of this type used a bright lamp to illuminate a smoke-laden flow. Later, Shaughnessy and Morton[3] found that using a laser as the illumination source improved the signal/noise ratio. By a system of lenses and slits, the scattering from a small volume of seeded gas was collected and focused onto a photomultiplier tube (PMT). The PMT output was then shown to be proportional to the seeded gas concentration, and it was possible to measure average concentration, concentration fluctuations, and power spectra at a single point. Our experiments invoke the same principle but, rather than measuring the time evolution of the concentration at a single point, the spatial concentration field is determined in two dimensions at a single instant, using a TV camera system.[4]

The Lorenz/Mie scattering process (i.e., scattering from particles with sizes on the order of the wavelength of light) is used for the results to be presented here. This is by far the strongest scattering mechanism available for this work and, since there are no chemical reactions present and the gas composition is known beforehand for the cases studied, the fact that the scattering mechanism is not sensitive to particular gas species is not critical.

Experimental Considerations

Light-Scattering Configuration

The experimental apparatus is shown schematically in Fig. 1. The gas introduced into an atomizing aerosol generator (Sierra Instruments Model 7330) is seeded with sugar particles (diameter <1 μm) and then directed into a 4-mm-diam axisymmetric jet. For the flow conditions present in this jet, other studies[5] indicate that particles of this size should easily follow the flow and, in addition, that their light-scattering properties should provide ample signal intensity. A sheet of illumination is formed by focusing the principal wavelengths (514.5 and 488 nm) of a 2.5 W cw argon-ion laser first with a long focal length spherical lens (1.5 m) and then diverging the focusing beam in one dimension with a cylindrical lens. The resulting sheet (0.15-mm thick) is directed through the center of the jet flow. The use of a sheet of illumination eliminates the "integrated" effects common in many flow-visualization experiments. The elastically scattered light from the aerosols in the illuminated sheet is then collected with a lens L_1 and focused onto the face of a computer-controlled, low-light-level TV camera by lens L_2. In order to freeze the turbulent motion, the TV camera is gated on by a high-voltage pulse generator for a period of 10 μs. The image is then digitized under computer control and the values are transferred to the computer memory and later to magnetic tape. For the results to be presented here, the images have been digitized in a 100×100 point format so that the scattered light intensity as a function of position is recorded for each of 10,000 points. The lenses L_1 and L_2 have been selected so that a 2×2 cm^2 area is imaged onto the active area of the TV camera. The illuminated volume corresponding to each digitized intensity is, therefore, $0.20 \times 0.20 \times 0.15$ mm. If the seeding density is controlled so that there is a large number of particles (about 1000) in this volume element, the scattered light intensity will be proportional to the concentration of the seeded gas in the volume element. (Note that this remains true only if molecular diffusion is negligible.) Therefore, each digitized image represents the instantaneous nozzle gas concentration as a

Presented as Paper 80-1370 at the AIAA 13th Fluid and Plasma Dynamics Conference, Snowmass Colo., July 14-16, 1980; submitted Sept. 18, 1980; revision received March 20, 1981.

*Assistant Professor, Dept. of Engineering and Applied Science.
†Professor, Dept. of Engineering and Applied Science.

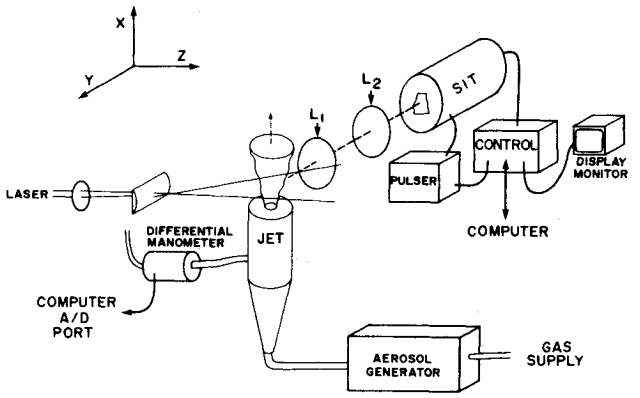

Fig. 1 Experimental configuration for the Lorenz/Mie scattering experiment. Elastically scattered light from a seeded flow is imaged onto a computer-controlled, low-light-level TV camera. The digitized intensities stored in the computer are proportional to the nozzle gas concentration distribution.

function of position in two dimensions. Many of these images can be stored and various statistical quantities calculated from them. Because the time required to digitize 10,000 points is about 1 s, successively digitized images are essentially independent events and statistical quantities calculated from them are ensemble-averaged rather than time-averaged.

Data Corrections and Noise Sources

The raw data from the TV camera stored on magnetic tape must be corrected in two ways. First, a "no-signal" frame is obtained and subtracted from each frame of data. (Here a frame is a 100×100 array of digitized points representing the image.) This corrects for the nonzero background in the data caused by dark noise in the camera, as well as the numerical offset inherent in the analog-to-digital conversion. For the second correction step, a rectangular cuvette containing a very dilute fluorescent dye solution is placed in the illuminated sheet. The scattered fluorescent radiation provides a "constant illumination" field which is then digitized and stored in the computer after the background frame has been subtracted. Each data frame is then divided by this uniform illumination frame. This process corrects for a number of things:

1) The illumination sheet is not really uniform. Since the sheet is formed from a laser with a somewhat Gaussian beam intensity profile, the intensity within the sheet tends to "fall off" toward the edges.

2) The response of the TV camera system tends to be greater in the center of the field of view than at the edges.

3) Vignetting in the collection optics can cause the image on the face of the TV camera to be dimmer near the edges.

All of these effects tend to give the digitized images anomalously large values near their centers. Dividing by the response frame, which is also peaked toward the center, tends to correct this. The correction scheme helps considerably; however, experience shows that the correction is not complete and that signals toward the center typically remain several percent higher than they should be.

When the flow is seeded with macroscopic particles (i.e., the Lorenz/Mie scattering case), the major source of noise is the so-called marker shot noise. This shot noise is due to the finite number of particles in each resolved volume element. To minimize this noise, it is desirable to have as many particles as possible in each volume element. Care must be taken, however, not to seed so heavily that secondary scattering becomes important, since the scattered radiation must travel through a medium made inhomogeneous by the turbulence in order to reach the collection optics. A guideline set forth by Shaughnessy and Morton[3] that the beam attenuation through the entire flow be less than 5% was followed. Another factor that limits the maximum seeding density is that if the flow is seeded too heavily, the effective density and viscosity of the gas can be affected. It has been seen that changes in the gas density can affect the spreading rate of the jet.[6] Therefore, the mass ratio of the seed particles to the gas was limited to a few percent.

In order to make accurate concentration measurements, a high seeding density is needed. While the aerosol generator used produces a sufficiently large number of particles for our purpose, the aerosols generated are polydispersed. Since the larger particles scatter radiation much more efficiently than the smaller ones, the use of a polydispersed aerosol for marking the nozzle fluid tends to worsen the problem of marker shot noise. Nevertheless, the intensity of the scattered radiation from a polydispersed aerosol may still be taken as proportional to the total number of particles in a scattering volume, providing that the particle size distribution in all such volumes is approximately the same.

Inherent in the use of aerosols as markers for studying turbulent mixing is the assumption that the particles are thoroughly mixed with the nozzle fluid before leaving the nozzle. To test the uniformity of the particle seeding, the nozzle fluid is piped through a rectangular glass cell where its concentration is monitored. Tests showed that the noise associated with nonuniform seeding is small compared to the marker shot noise.

Flow System

As stated earlier, the jet used for these experiments has a diameter of 4 mm. The relatively small diameter was chosen to make it possible to collect the scattered light efficiently with commercially available camera lenses. The design was patterned after those used in similar experiments described in a review by Harsha.[7] The seeded gas enters the jet and passes through an expansion section, three wire meshes, and into the plenum chamber. The diameter of the plenum is 5.8 cm, which gives a contraction ratio of 211. The transition to the final 4-mm diam exit aperture is a smooth contour which prevents flow separation and recirculation.

Hot-wire measurements were made to check the velocity profiles and to characterize the flow. The rms freestream turbulence at the jet exit was measured to be 0.13% of the nozzle velocity. In order to prevent accumulation of aerosol particles in the ambient gas, the jet was enclosed in a large chamber exhausting at the top. The ratio of the jet exit velocity to the velocity of the ambient air was maintained at greater than 120. For the results presented here and in Ref. 8, the boundary layer at the nozzle exit is laminar. A more detailed description of the flow conditions is also given in Ref. 8.

Experimental Results

Data Interpretation

The motion of a small particle in a fluid may be expressed by

$$m \frac{dv}{dt} = c_f(u-v) + f$$

where m is the effective mass of the particle, v the particle velocity, u the fluid velocity, c_f the friction coefficient, and $c_f(u-v)$ the mean force exerted by the moving fluid on the particle. The quantity f denotes the rapidly fluctuating stochastic force resulting from molecular agitation. For micron-sized sugar aerosols in air, the effective mass of individual aerosol particles may be taken as the actual mass of the particle. The equation clearly shows that the velocity of the particles lags behind the flow velocity, and the "velocity slip" is characterized by a relaxation time $\tau = m/c_f$. For the aerosols used, c_f may be taken as $3\pi\mu d_p$ in accordance with Stokes' law, where μ is the viscosity of air and d_p the aerosol diameter. Hence

$$\tau = \frac{\pi}{6} \rho_p d_p^3 \Big/ (3\pi\rho\nu d_p) = \frac{1}{18} \frac{\rho_p}{\rho} \frac{d_p^2}{\nu}$$

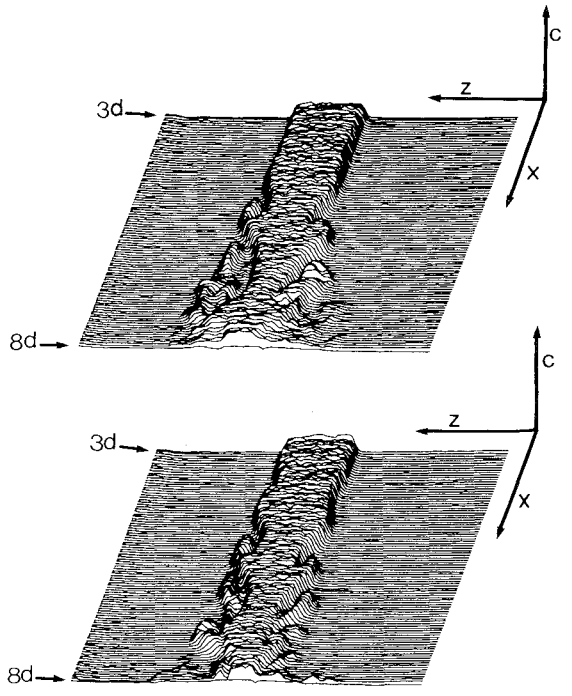

Fig. 2 Instantaneous nozzle fluid concentration in the x-z plane. Height above the x-z plane, which intersects the jet axis, represents concentration.

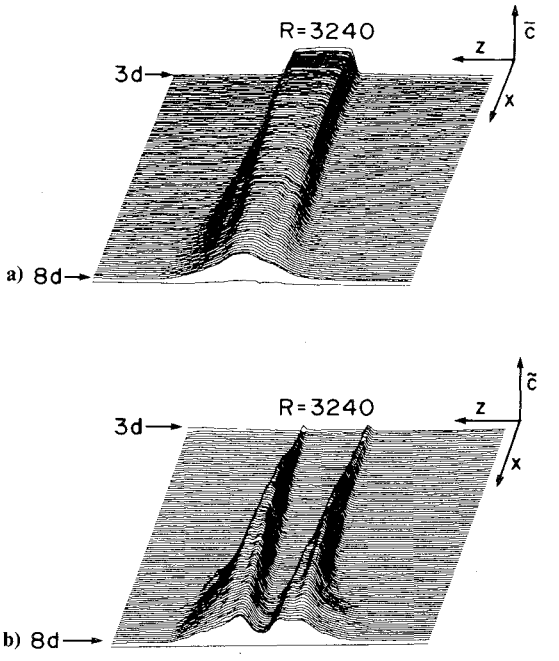

Fig. 3 a) Average concentration and b) rms concentration fluctuations for an axisymmetric jet at a Reynolds number of 3240, both calculated from the same set of 1000 realizations.

where ρ_p/ρ is the ratio of the density of the aerosol to the density of the air (~ 1000) and ν is the kinematic viscosity of air. For a 1-μm particle, $\tau = 3.7 \times 10^{-6}$ s. The displacement lag is of the order $\tau \Delta U$, so for a jet speed of 15 m/s, the maximum displacement lag is about 56 μm, which is smaller than the smallest scale that can be resolved by our system in this study (0.20 mm).

The effect of the stochastic fluctuating force is to produce a Brownian diffusion of particles with a diffusivity given by Einstein[9]:

$$D = kT/c_f$$

where k is the Boltzmann constant and T the absolute temperature. For our aerosols at room temperature, D is about 2.4×10^{-8} cm^2/s. During the time the aerosols are carried a distance L by the fluid moving at a velocity U, the particles would have diffused a distance on the order $\sqrt{2D(L/U)}$. If we take L to be 10 nozzle diameters and U to be 15 m/s, this distance is about 0.1 μm, and the displacement of particles due to diffusion is completely negligible.

Clearly then, for studying turbulent mixing, the motion of the nozzle fluid is faithfully marked by the aerosol particles. On the other hand, in a region where the transport is mainly controlled by molecular diffusion, it would be altogether misleading to infer the distribution of nozzle fluid from the Lorenz/Mie scattering technique. If scattering mechanisms sensitive to the molecules themselves are used to determine the fluid concentration, the effect of molecular diffusion can be studied (see the section on other scattering mechanisms at the end of this paper).

In all our measurements, the smallest resolvable scale is 0.2 mm so that the size of the smallest detectable turbulent eddies is somewhat larger than 0.2 mm. This is generally larger than the smallest turbulent scales in the region of the flow where the data are gathered. For example, in a jet discharging from a 4-mm nozzle at a Reynolds number of 4000 (a flow speed of 15 m/s), the turbulent microscale at 10 diam downstream of the nozzle exit is 0.08 mm and in the mixing layer the scale is even smaller. Our system, therefore, is best suited for studying large-scale turbulent mixing in regions where the macroscale is much greater than 0.2 mm while the microscale may be much less.

Since turbulent eddies are transported by the flow, the most rapidly varying components of the fluctuation are contributed by the smallest eddies. The highest frequency associated with the smallest detectable eddies at a flow speed of 15 m/s is about 7.5 kHz. This corresponds to a time scale of 130 μs for the most rapid detectable change. Consequently, when the TV camera is gated on for 10 μs, one effectively obtains a record of the instantaneous distribution of the nozzle fluid in the flow.

Instantaneous Realizations

Once the images from a particular set of flow conditions have been digitized and stored on tape, it is possible to review and analyze them in many different ways. The capability to examine the many individual instantaneous realizations is essential for correctly interpreting and understanding the various statistical averages. To this end, a computer-controlled display monitor is available for quick visualizations of the stored data and a digital plotter provides a "hard-copy" capability. One of the ways of plotting the data is shown for two independent realizations in Fig. 2. In this figure, x is the distance downstream, z the distance radially across the jet, and the x-z plane passes through the jet axis. The height above the x-z plane represents the scattered light intensity which is directly proportional to the nozzle gas concentration. The region covered is a 2×2 cm^2 area corresponding to the region from 3 to 8 jet diameters downstream. The Reynolds number is 3240. The existence of large-scale coherent structures is easily seen in these representations.

Average Concentration and rms Fluctuations

One of the very basic quantities that can be calculated from a set of instantaneous digitized images is the average concentration as a function of downstream distance x, and the distance across the jet z. The ensemble average is calculated by

$$\bar{C}(x,z) = 1/N \sum_{i=1}^{N} C_i(x,z)$$

where N, the number of instantaneous realizations, is 1000, and $C_i(x,z)$ is the ith instantaneous concentration distribution

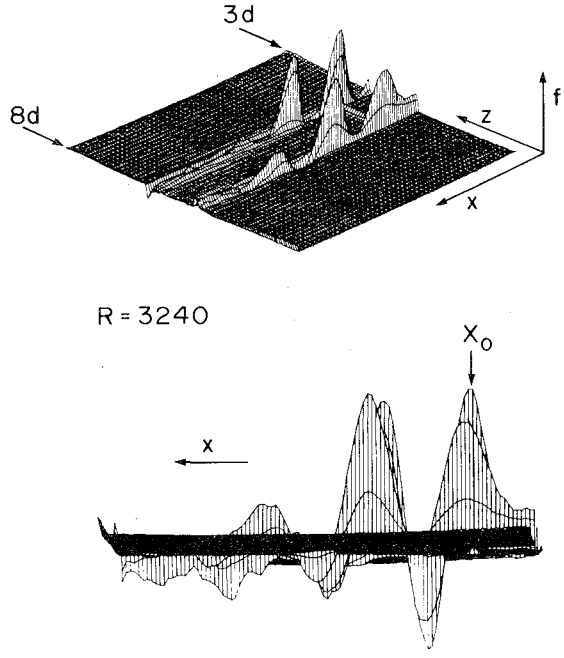

Fig. 4 Two different views of the covariance field of the concentration fluctuations in the streamwise direction, x, for a Reynolds number of 3240. The fixed point x_0 was arbitrarily chosen to be about 4 diameters downstream.

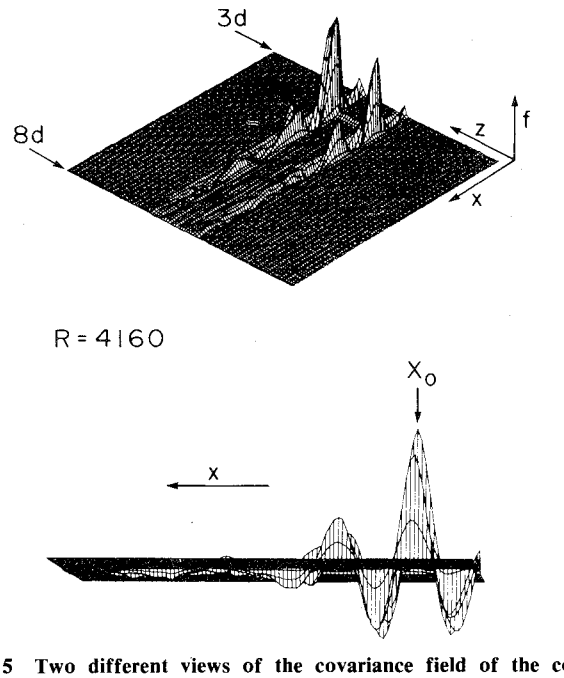

Fig. 5 Two different views of the covariance field of the concentration fluctuations in the streamwise direction x for a Reynolds number of 4160. The fixed point, x_0, was arbitrarily chosen to be about 4 diam downstream. Note the difference in the length scales (peak separations) from those in Fig. 4.

corrected for background and camera response as described earlier. Figure 3a shows the average concentration for the region between 3 and 8 jet diameters downstream for a jet with Reynolds number of 3240 (based on the nozzle diameter and jet velocity).

Once the average concentration has been obtained, the instantaneous concentration fluctuation $C_i'(x,z)$ can be calculated by subtracting the average concentration from the ith instantaneous realization as follows:

$$C_i'(x,z) = C_i(x,z) - \tilde{C}(x,z)$$

Given this, the rms concentration fluctuation, $\tilde{C}(x,z)$, can be calculated as

$$\tilde{C}(x,z) = 1/N\left\{\sum_{i=1}^{N} C_i'(x,z)^2\right\}^{1/2}$$

where $N=1000$. The results of this type of calculation are shown in Fig. 3b for the same flow conditions. Note that at several downstream locations in the mixing layer on both sides of the jet, the rms concentration fluctuation has two maxima separated by a slight local minimum (looking in the z direction). Comparison with Fig. 3a shows that the regions displaying this "double peak" behavior in the rms fluctuations correspond to those locations on either side of the jet where the average concentration has triple inflection points. This behavior has been observed by others[10] in similar flowfields.

Spatial Covariances

While the average concentration and rms concentration fluctuations presented in the previous section are important parameters and allow us to compare our results with the work done by others, some significant advantages of the technique have not been utilized. In principle, it would have been possible to obtain these quantities by a series of tedious point-by-point measurements. However, the fact that 10,000 measurements of the concentration field are made, *simultaneously* makes it possible to obtain statistical quantities regarding the spatial characteristics of the flow. An example is the covariance of the concentration fluctuation taken along lines in the streamwise direction as shown in Fig. 4. A fixed point, x_0, is selected at an arbitrary distance downstream and the covariance calculated relative to it using the form

$$f(x,z) = 1/N\sum_{i=1}^{N} C_i'(x,z)\,C_i'(x_0,z)$$

where, as before, $N=1000$ and $C_i'(x,z)$ is the concentration fluctuation for the ith instantaneous realization. In Fig. 4, the $f(x,z)$ surface is plotted from two different angles to show all features. Note that the peak at $x=x_0$ is simply the mean square concentration fluctuation at that point. The other positive and negative peaks correspond to the correlation and anticorrelation of features in the flow. The spacing between these peaks gives a measure of the average spacings of the large coherent structures seen in the instantaneous data (e.g., see Fig. 2). The width of the peaks is an indication of the average size of these structures and the height of the peaks provides information on the coherence of the structures. Figure 5 shows $f(x,z)$ for the same two views for the higher Reynolds number case. The peaks are less pronounced here and the spacing is slightly different. The length scales characteristic of the flow, which can be obtained by measuring the distance between peaks, are important input parameters for some models of turbulence (e.g., see the review by W. C. Reynolds[11]). Obtaining this parameter is possible because of the simultaneous multipoint detection capabilities inherent in the TV camera measurement system.

To obtain a clear comparison between the covariance data for the two different Reynolds number cases, Fig. 6 shows the values of $f(x,z_0)$ and $f(x,z_1)$ for $R=3240$ and 4160. Here z_0 and z_1 correspond to the radial position where $f(x,z)$ has the largest values. For the lower Reynolds number, the structures remain correlated to some extent over the entire region shown, while at the slightly higher Reynolds number, the correlation dies out at about $x=6d$. The length scales, which are shorter for $R=4160$, seem to be quite similar on both sides of the jet, although at $R=3240$ the details of the covariance are quite different near $x=7d$. It is interesting to note that

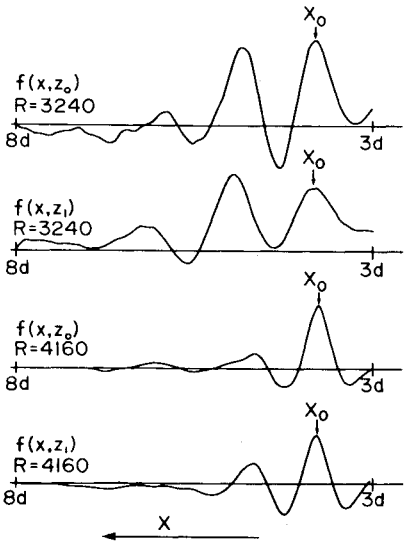

Fig. 6 Covariance in the streamwise direction x shown for specific radial positions, z_0 and z_1, which correspond roughly to the edges of the jet. The top two are for a Reynolds number of 3240; the bottom two have $R = 4160$.

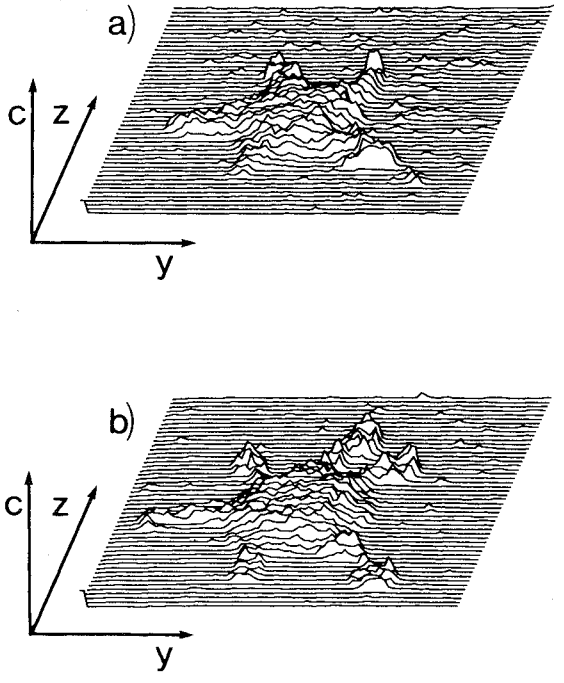

Fig. 7 Instantaneous nozzle fluid concentration in the y-z plane. Both (a) and (b) were obtained at the same distance from the nozzle and at the same flow velocity. Instabilities in the vortex ring structures cause the lobed appearance.

since $f(x,z)$ is not normalized, the value of $f(x_0,z)$ for a given z is not necessarily the largest. (The covariance is calculated relative to the fixed point x_0 as before.) This can be seen to be the case in $f(x,z_1)$ for the lower Reynolds number (Fig. 6). This behavior can be expected if the disturbances are amplified as they are carried downstream.

Measurements Normal to the Jet Flow

By changing the orientation of the illumination sheet with respect to the jet, it is possible to investigate the behavior of the flow in the plane normal to the flow direction. Referring to Fig. 1, this is the y-z plane; the flow is still in the x direction. Instantaneous concentration maps obtained in this way are shown in Fig. 7. The data were obtained from a jet of preliminary design with a diameter d of 2 mm. The Reynolds

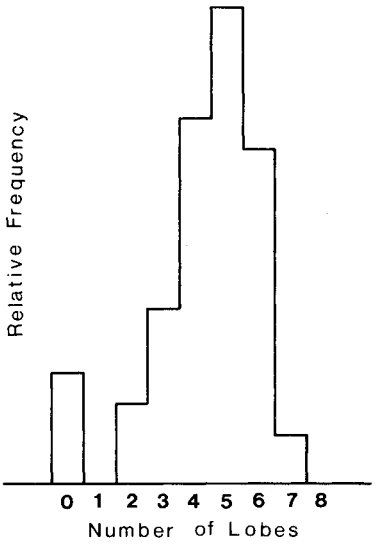

Fig. 8 Relative frequency of the number of lobes in large-scale structures. The result was obtained from 100 instantaneous realizations of the concentration measured normal to the jet flow. The data were taken 6 jet diameters downstream at a Reynolds number of 2300.

number was about 2300 and the downstream distance was $6d$ for the two realizations. Although the flow conditions are the same, the instantaneous concentration distributions are quite different, with one showing a five-lobed structure and the other a differently oriented six-lobed configuration. This type of structure is believed to be a manifestation of the instability of vortex rings to azimuthal disturbances. According to Widnall and Sullivan,[12] the number of lobes present depends on the ratio of the radius of the vortex core to the radius of the ring. Examining other instantaneous maps taken under the same conditions reveals the presence of two-, three-, four-, five-, six-, and seven-lobed structures. The number of lobes was determined by visual inspection for each of 100 instantaneous realizations. The distribution obtained (shown in Fig. 8) is seen to peak with five lobes as the most common number. For these flow conditions, more than 90% of the instantaneous maps had some lobed structure and about 30% had five lobes.

More recent experiments on other jet flows reveal that the ensemble-averaged quantities (1000 realizations) do not have strict circular symmetry in the region where the lobed structures are observed. While the lobes are by no means stationary in space, they do seem to be more likely to occur in certain preferred orientations relative to the nozzle. When the nozzle is rotated 90 deg, the asymmetries in the averaged distributions are also, indicating that the preferred orientation of the lobed structures is more or less fixed by microscopic biases inside the nozzle.

Temporal Information

As previously mentioned, the time required to digitize 10,000 points and record them on magnetic tape is long compared to the characteristic time in the flow. This makes it impossible to measure the time history of the flow in a straightforward manner. Temporal information can be obtained, however, if some modifications are made to the experimental setup. Since the TV camera essentially measures the intensity of incident radiation as a function of two variables, we have some leeway as to which two variables we choose. For example, a time variable can be substituted for one of the spatial variables and intensity measured as a function of distance x and time t. A schematic diagram of how this can be done in the context of the current experiment is shown in Fig. 9. Rather than forming a sheet of illumination, the laser is focused into a line and the line is directed into the mixing layer of the jet. The addition of a rotating mirror between the collection lens, L_2, and the focusing lens, L_3, allows the image of the line to be swept across the face of the camera as a function of time. The camera is gated on for the entire time the image of the line is

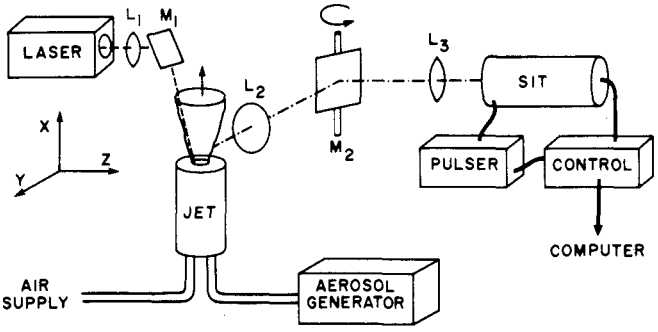

Fig. 9 Experimental configuration used to obtain the time evolution of nozzle gas concentration along a line within the mixing region. A rotating mirror sweeps the image of the line across the face of the TV camera in time.

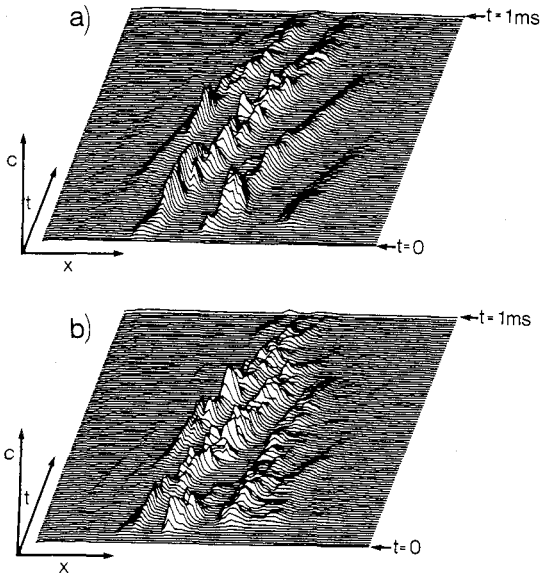

Fig. 10 Concentration as a function of downstream distance x and time t. The slope of the structures in the x-t plane gives the velocity of the large-scale structures. (No correction has been made for vignetting or camera response and, therefore, the signal drops off considerably toward the edges in both frames.)

crossing the active part of the detector. The digitized values are then a representation of $C(x,t)$. Figure 10 shows two sets of data obtained in this manner.

The data on $C(x,t)$ give several kinds of information. The trajectories of the large structures in the mixing layer are clearly traced out. The slope of these trajectories in the x-t plane gives the speed of convection of the structures. Figure 10b shows that in some cases the structures can have velocities relative to one another and therefore coalesce and interact. According to Winant and Browand,[13] this coalescence of the large-scale structures and the pairing of vortices is an important mechanism in turbulent mixing. The mean convection speed of the large structure, as determined from Fig. 10, is on the order of one-half of the jet velocity. It is also clear that the structures are changing internally as they are carried downstream, as evidenced by the varying concentration levels within each trajectory. This behavior is expected if the structures consist of vortices that form and, in time, become unstable.

Other Scattering Techniques

In some flow systems where it would be highly desirable to obtain simultaneous multipoint measurements of gas concentration, the limitations imposed by the necessity of seeding make the Lorenz/Mie scattering technique unacceptable. Some examples of these are:

1) Chemically reacting flows. To study the interaction between turbulence and chemical reactions, it would be desirable to measure the concentration of fuel, oxidizer, and combustion products separately. The nonspecific character of the Lorenz/Mie technique in distinguishing different species does not allow this.

2) High-speed flows. As flow velocities approach and exceed the speed of sound, it becomes increasingly difficult to be certain that seed particles will be able to follow the details of the flow in regions of high local acceleration.

3) Flows in which molecular diffusion plays a significant role. Because of the difference in the mobility of the molecules and the seed particles, any mixing due to molecular diffusion will be missed by detecting scattered light from the relatively large particles. While this is thought to be a minor effect for large-scale mixing, this is certainly not true for the small-scale mixing or for very low Reynolds number flows.

4) Flows in which very high spatial resolution is desired. As mentioned earlier, the major source of noise for the Lorenz/Mie scattering technique is marker shot noise caused by the finite number of particles in a particular volume element. As the size of this volume element decreases, the marker shot noise increases and, in most cases, the seeding level cannot be increased proportionally. Therefore, to study the smallest scales in the flow, which for the jet used in the current study are smaller than the resolution by a factor of ten, the noise due to finite seeding would be very large. This can also be a problem when looking at flows, such as the axisymmetric jet in the far-field region, where significant mixing has occurred (and, therefore, reduction of the number density of seed particles).

For such flow situations, scattering mechanisms that are sensitive to the molecules of the flow themselves become desirable. With the variety of laser sources currently available, the experimental configuration for the Lorenz/Mie experiment should be applicable to studies utilizing these other scattering processes. For example, the concentration will be proportional to the fluorescence intensity if the nozzle gas is seeded with a fluorescing molecular species such as iodine vapor. If a slightly more powerful laser source is available, the scattered fluorescent radiation will be sufficient for TV camera detection. Other species-sensitive scattering processes, such as Rayleigh scattering (elastic scattering from molecules) or Raman scattering (inelastic scattering from vibrational states of molecules), are much weaker but have been used successfully for single-point concentration measurements and are being pursued as the scattering mechanism for measuring gas concentrations simultaneously in two dimensions.

Conclusions

A light-scattering technique which makes it possible to map out the instantaneous concentration field at 10^4 points in a thin sheet intersecting a nonreacting turbulent flow is described. The technique is adapted to study large-scale turbulent mixing using the Lorenz/Mie scattering mechanism. Typical experimental results that may be obtained by this method are shown. A more detailed study of the fluid dynamic implications from this investigation may be found in Ref. 8. The limited spatial resolution imposed by the Lorenz/Mie scattering mechanism may be eelaxed when other scattering mechanisms are used in combination with the technique.

Acknowledgment

We thank the Office of Naval Research, Project SQUID, for partial support of this work under Contract No. N00014-79-C-0254.

References

[1] Rosensweig, R. E., Hottel, H. C., and Williams, G. C., "Smoke-Scattered Light Measurements of Turbulent Concentration Fluctuations," *Chemical Engineering Science*, Vol. 15, July 1961, pp. 111-129.

[2] Becker, H. A., "Mixing, Concentration Fluctuations, and Marker Nephelometry," *Studies in Convection,* Vol. 2, edited by B. E. Launder, Academic Press, New York, 1977, pp. 45-139.

[3] Shaughnessy, E. J. and Morton, J. B., "Laser Light-Scattering Measurement in a Turbulent Jet," *Journal of Fluid Mechanics,* Vol. 80, April 1977, pp. 129-148.

[4] Long, M. B., Webber, B. F., and Chang, R. K., "Instantaneous Two-Dimensional Concentration Measurements in a Jet Flow by Mie Scattering," *Applied Physics Letters,* Vol. 34, Jan. 1979, pp. 22-24.

[5] Agarwal, J. K. and Fingerson, L. M., "Evaluation of Various Particles for Their Suitability as Seeds in Laser Velocimetry," *Laser Velocimetry and Particle Sizing,* edited by H. D. Thompson and W. H. Stevenson, Hemisphere Publishing Corp., Washington, 1979, pp. 50-63.

[6] Webber, B. F., Long, M. B., and Chang, R. K., "Two-Dimensional Average Concentration Measurements in a Jet Flow by Raman Scattering," *Applied Physics Letters,* Vol. 35, July 1979, pp. 119-121.

[7] Harsha, P. T., "Free Turbulent Mixing: A Critical Evaluation of Theory and Experiment," AEDC-TR-71-36, 1971.

[8] Long, M. B. and Chu, B. T., "On the Mixing Mechanism and Structure of an Axisymmetric Turbulent Mixing Layer," *AIAA Journal,* Vol. 19, Sept. 1981, pp. 1158-1163.

[9] Einstein, A., "On the Movement of Small Particles Suspended in a Stationary Liquid Demanded by the Molecular Kinetic Theory of Heat," *Annalen der Physik* (Leipzig), Vol. 17, 1905, pp. 549-560; also *Investigations on the Theory of the Brownian Movement,* Dover ed., 1956, pp. 1-35.

[10] Fiedler, H. E., "On Turbulence Structure and Mixing Mechanism in Free Turbulent Shear Flows," *Turbulent Mixing in Nonreactive and Reactive Flows,* edited by S. N. B. Murthy, Plenum Press, New York, 1975, pp. 381-409.

[11] Reynolds, W. C., "Computation of Turbulent Flows," *Annual Review of Fluid Mechanics,* Vol. 8, 1976, pp. 183-208.

[12] Widnall, S. E. and Sullivan, J. P., "On the Stability of Vortex Rings," *Proceedings of Royal Society of London,* Series A, Vol. 332, 1973, pp. 335-353.

[13] Winant, C. D. and Browand, F. K., "Vortex Pairing: The Mechanism of Turbulent Mixing-Layer Growth at Moderate Reynolds Number," *Journal of Fluid Mechanics,* Vol. 63, 1974, pp. 237-255.